RSC Advances

ROYAL SOCIETY OF CHEMISTRY

www.rsc.org/advances

RSC Advances

PAPER

Label-free electrochemical detection of DNA methyltransferase activity via DNA tetrahedron-structured probe†

Received 00th January 2016,
Accepted 00th January 2016

DOI: 10.1039/x0xx00000x

www.rsc.org/advances

Hongyu Zhao,[‡a] Hai Yin[‡b] and Yongfeng Yang[*a]

Recently, 3-dimension DNA nanostructures have been gained significant attention due to their programmable folding nature. Herein, DNA tetrahedron-structured probe (DTP) is designed for detection of methyltransferase (MTase) activity based on HRP-mimicking DNAzyme triggered deposition of polyaniline (PANI). In this strategy, MTase activity is measured with differential plus voltammetry (DPV) by using PANI as the redox label. Furthermore, the DNA tetrahedron controlled the nanospacing between capture DNA, which greatly improves hybridization efficiency, MTase combination capability, and detection sensitivity. Using this method, more than 5 times higher signal gain is achieved compared with single-strand capture DNA probe (ssP) without the tetrahedron structure. Under optimized experimental conditions, the DPV intensity is in linear correlation with M.SssI concentration ranging from 0.05 to 10 U/mL, with a correlation coefficient of 0.9936 and a detection limit of 0.03 U/mL (S/N = 3). The inhibition of 5-Aza-z'-deoxycytidine or procaine on M.SssI activity is also evaluated. Good accuracy, precision and sensitivity are obtained when the method is applied in complex matrix such as human serum samples, which is significant for clinical diagnosis and drug development.

1. Introduction

DNA methyltransferase (MTase) is an important subclass MTase. It includes the S-adenosylmethionine (SAM) binding site, a vicinal proline-cysteine pair which forms a thiolate anion important for the reaction mechanism, and the cytosine substrate binding pocket. MTase transfers a methyl group from the methyl group donor of SAM to the C5-positon of cytosine or the 6-amino group of adenine at specific base sequence.[1] It plays a significant regulatory role in both prokaryotes and eukaryotes.[2,3] The activity of MTase influences DNA methylation level, and the abnormity of DNA MTase activity is related to embryonic development,[4] cancer growth,[5,6] aging,[7] and cancer therapy.[8] Because of its key role in pathology and diagnostics, analysis of DNA MTase activity has been increasingly received research interests.

In recent years, various strategies have been developed for the determination of DNA MTase activity, including colorimetry,[9] fluorometry,[10] chemiluminescence,[11] However, each of them still has its limitations including low sensitivity, complicated manipulation, time-consuming or need elaborate instruments and expensive fluorescent substances. Electrochemical technology has been the most extensively used research method due to its own merits of high sensitivity, simplified setup, and low cost.[12,13] More recently, several electrochemical MTase activity assays have been proposed. For example, Qiu's group employed graphene oxide/gold nanoparticles/luminol composites to quantify DNA adenine methylation (Dam) MTase.[14] Chen's group developed an electrochemical biosensor to detect MTase activity based on electrocatalytic oxidation of ascorbic acid by graphene.[15] However, the simplicity, robustness, and sensitivity of the reported electrochemical MTase activity assays are not entirely satisfactory. To better apply DNA MTase to early diagnose interrelated diseases, further efforts are needed in the development of simple and sensitive MTase activity assays.

3-dimension DNA nanostructures, which have programmable folding nature, have been gained significant attention. Owing to their highly specific Watson-Crick base pairing, DNA molecules can be self-assembled into DNA nanostructures of various sizes, shapes, and geometries with high predictability and precision.[16–18] For example, DNA tetrahedron-based sensor was applied to the detection of DNA, which greatly increased target accessibility and reactivity.[19–23] Polyaniline (PANI) holds great promise in electrochemical sensor, due to its high electrical conductivity, easy producibility, environmental stability, relatively low cost, redox property and reversible nature of electrical conductivity.[24,25] Horseradish peroxidase (HRP) enzyme could efficiently catalyze oxidation polymerization of aniline to PANI in the presence of H_2O_2. However, the major drawback accompanying the HRP-catalyzed reaction is that complicated fabrication and easily losing catalyzed activity of HRP limit its further wide application. Recently, HRP mimicking DNAzyme have been substituted for HRP to catalyze the PANI deposition, due to its advantages of simple, environmentally benign, higher degree of control over the kinetics of the reaction, and avoiding complex and expensive chemically conjugated procedures.[26–29]

[a] The Second Hospital of Nanjing, Affiliated to Medical School of Southeast University, Nanjing, 210003, China
[b] Chinese People's Liberation Army 454 Hospital, Nanjing, 210001, China
‡ Hongyu Zhao and Hai Yin have contributed to this work equally.
Electronic Supplementary Information (ESI) available: experimental section. See DOI: 10.1039/x0xx00000x

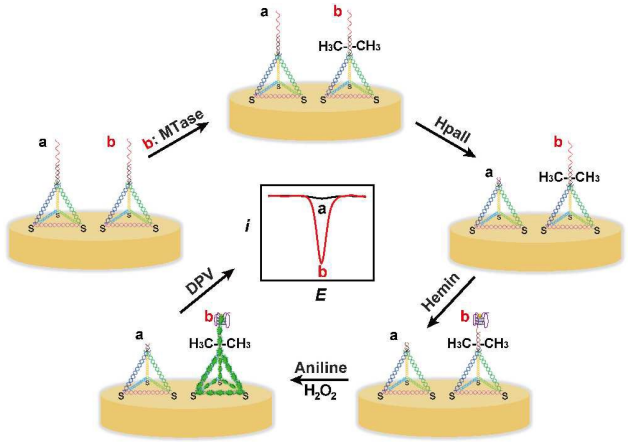

Scheme 1 Schematic illustration of label-free electrochemical detection of DNA methyltransferase activity via DNA tetrahedron-structured probe.

In this study, we developed a label-free electrochemical platform for assay DNA MTase activity by using DNA tetrahedron-structured probe. Compared with single-strand capture DNA probe (ssP), more than 5 times higher current was obtained by using tetrahedron DNA nanostructured probe. Because the tetrahedron DNA nanostructure could not only control the nanospacing between capture DNA which led to a better hybridization efficiency and MTase combination capability but also supply plenty of nucleic acid backbones for PANI deposition. In addition, the proposed method has been used to evaluate and screen the inhibition of MTase activity. It is expected that the proposed biosensor has the potential to be applied for cancer diagnosis and drug development.

2. Results and discussion

Analytical principle for MTase detection

Scheme 1 illustrated a schematic of the strategy for MTase detection. Firstly, the capture DNA, containing a 5′-CCGG-3′ sequence for methylation, was designed on top of the DNA tetrahedron, which was constructed by four DNA strands (tetra-A, B, C, and D, Table S1). Then the DTP was immobilized on the surface of the gold electrode via gold-sulfur affinity. In this way, the top capture DNA was stably raised upright followed by hybridizing with the target DNA which had a G-rich sequence. In the presence of HpaII, the intact 5′-CCGG-3′ sequence was recognized and cleaved. In this way, target DNA was removed from the electrode and no DPV signals was detected (Route a, Fig. 1, curve a). On the contrary, the second C base in the 5′-CCGG-3′ sequence was methylated by M.SssI in the presence of SAM, which could not be cleaved by HpaII. As a result, the G-rich sequence could be converted to HRP-mimicking DNAzyme in the presence of hemin and potassium ions.[30] This DNAzyme could catalyze the deposition of PANI on the electrode surface, leading to a readily measurable “turn-on” electrochemical signal. (Route b, Fig. 1, curve b).

Characterization of the assembling process

Surface plasmon resonance (SPR) is usually employed to investigate the specific binding of a target biomolecule or the formation of

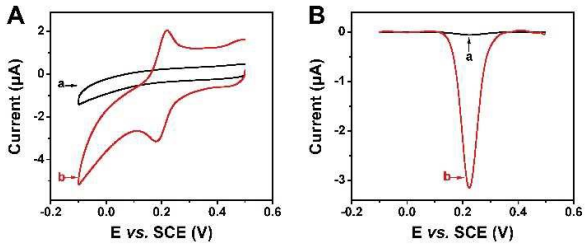

Fig. 1 CV (A) and DPV (B) of the gold electrode before (a) and after (b) methylation.

polymer on the surface of various modified substrates. The resonance angle is changed in positively proportional to the mass combined on the metal surface, which is used to ascertain the multiple coupling process. The modification and aniline polymerization on the chip were performed off-line. The surface was extensively rinsed with 1×PBS after each modification for eliminating the interference of physical adsorption. Fig. 2A gave the changes of SPR signal as a function of scanning angle on SPR chips with different modification stages. The resonance angles of the bare chip (Fig. 2A, curve a), DTP modified chip (Fig. 2A, curve b), HRP-mimicking DNAzyme/DTP modified chip (Fig. 2A, curve c) were 64.05°, 65.02°, and 65.47°, respectively. PANI modified chip (Fig. 2A, curve d) had higher resonance angles of 66.79°. These angles increased with the stepwise modifications, suggesting the successful assembling of DTP, the formation of HRP-mimicking DNAzyme, and the deposition of the PANI on the chip surface.

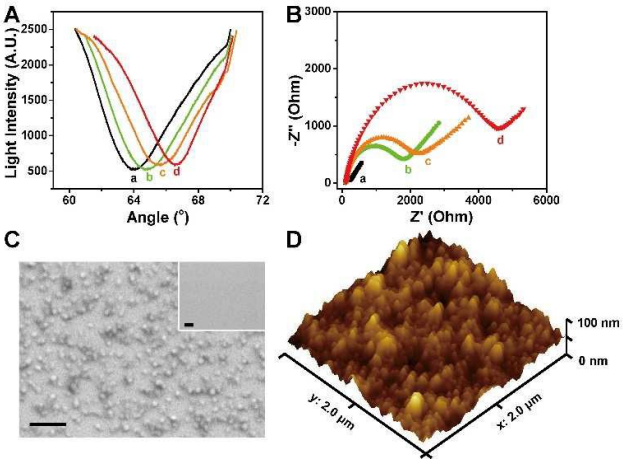

Fig. 2 Characterization of the modification process and the morphology of PANI on electrode surface. (A) SPR of bare chip (a), DTP modified chip (b), HRP-mimicking DNAzyme/DTP modified chip (c), and PANI modified chip (d). (B) EIS of bare gold electrode (a), DTP modified gold electrode (b), HRP-mimicking DNAzyme/DTP modified gold electrode (c), and PANI deposition on gold electrode (d). (C) Representative SEM image of PANI deposition on gold substrate. The inset showed a representative TEM image of bare gold substrate. The scale bars indicated 200 nm. (D) Representative AFM image of PANI deposition on gold substrate. Error bars show the standard deviation of three experiments.

Electrochemical impedance spectroscopy (EIS) is a powerful electrochemical technique for probing the features of surface-modified electrodes, which provides useful information on the impedance changes of the electrode surface during the fabrication process.[31] The bare gold electrode exhibited a nearly straight line in the Nyquist plot impedance spectroscopy (Fig. 2B, curve a), which indicated a very low electron-transfer resistance of the redox probe. After the continuous modification of DTP and HRP-mimicking DNAzyme, electron-transfer resistance (R_{et}) values increased stepwise (Fig. 2B, curve b, c) because of the negative charges of DNA prevented repelling electrons from approaching the electrode surface. After the polymerization of PANI onto the electrode, a large increasing R_{et} was observed (Fig. 2B, curve d), suggesting the formation of PANI further inhibited the interfacial electron transfer.[32]

The scanning electron microscopy (SEM) and atomic force microscopy (AFM) were taken to investigate changes of the surface morphology of the gold electrode during the assembling process of the biosensor construction. By comparison with a relatively clean and smooth surface of the bare gold substrate (insert in Fig. 2C), we could find an obvious change on the electrode surface after the deposition of PANI. The nanostructured PANI could be seen clearly on the gold electrode (Fig. 2C). Corresponding to SEM images, the deposition of PANI were also showed clearly in AFM (Fig. 2D).

All these experiments proved the self-assembled DNA nanostructure, HRP-mimicking DNAzyme formation and the deposition of PANI clearly.

DPV signal behaviors of different sensing strategies

The limited space available in nanosensors restricts the effective (hybridizable) number of immobilized probe molecules, which reduces the probability of collision and binding of the probe and target molecules.[33] Enlarging the nanospacing would be a benefit to the probe and target DNA binding. To verify our hypothesis and to improve the sensitivity, two MTase sensors with different probes were investigated for the analysis of MTase, including ssP and DTP. 2.5 U/mL M.SssI was analyzed by both ssP and TSP sensor. Meanwhile, 1×PBS was analyzed as blank. It was found that the DPV intensity from the DTP biosensor increased 5 times from that with ssP sensor (Fig. 3). One reason was that highly ordered DNA tetrahedron could resist the MTase absorption and regulate the nanospacing between the capture DNA (~ 5.0 nm).[23] All individual capture DNA tethered on the DNA tetrahedron immobilized orderly away from the gold electrode surfaces, leading to high hybridization efficiency and MTase combination capability. In contrast, ssP immobilized on the gold electrode surfaces were in a random fashion, which undergo complications and steric hindrance,[34] resulting in the hybridization efficiency and MTase combination decrease. More importantly, in this strategy, tetrahedral-structure probe supplied abundant nucleic acid backbones for aniline polymerization, which also increased the DPV signal sharply. Overall, the results of the sensor investigation were exactly consistent with our prediction.

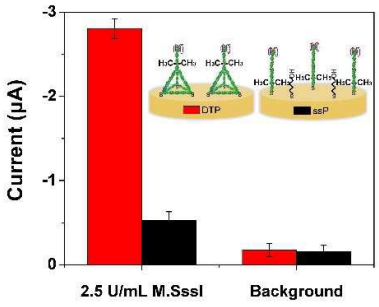

Fig. 3 DPV signal behaviors of DTS and ssP. A 1×PBS buffer was used as the blank. Error bars show the standard deviation of three experiments.

Detection of DNA MTase activity

The DNA MTase Activity was subsequently evaluated by the proposed approach to validate the sensitivity of this strategy. The change of DPV intensity with the various concentrations of M.SssI was investigated. DTP/target DNA hybrids were methylated with various concentrations of M.SssI (0 ~ 20 U/mL) for 3 h followed by incubation with HpaII for 3 h. The DPV intensity gradually increased with the increment of M.SssI concentration in the presence of DTP (Fig. 4A). This is due to the fact that more hybrids are methylated at higher concentration of M.SssI, which protected hybrids from being cleaved by HpaII. The DPV intensity was in log-linear correlation with M.SssI concentration (Fig. 4B, a). The dynamic range was from 0.05 to 10 U/mL with a good correlation coefficient of R^2 = 0.9936

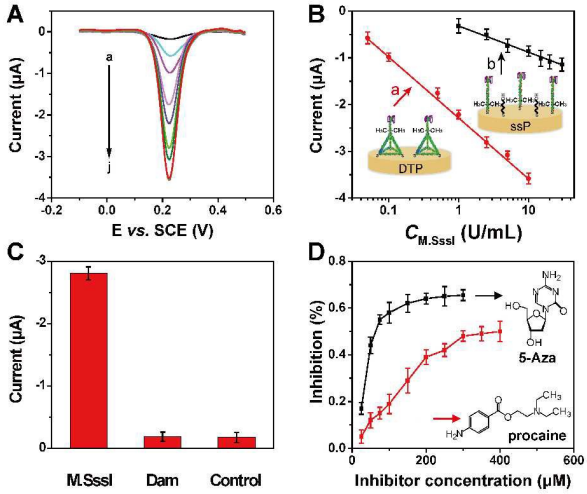

Fig. 4 (A) DPV corresponding to the biosensor treated with different concentrations of M.SssI MTase at (a) 0, (b) 0.05, (c) 0.1, (d) 0.5, (e) 1, (f) 2.5, (g) 5, (h) 10, (i) 15, and (j) 20 U/mL, respectively. (B) The linear plot of DPV current versus the logarithm of M.SssI MTase ranging from 0.05 to 10 U/mL using DTP probe (a) and 1 to 30 U/mL using ssP probe (b). (C) Selectivity of the sensing system. The concentration of both M.SssI and Dam MTase is 2.5 U/mL. (D) The inhibition effect of 5-Aza and procaine on M.SssI MTase activity. Error bars show the standard deviation of three experiments.

and detection limit of 0.03 U/mL (S/N = 3). In contrast, the biosensor with ssP exhibited a detection limit of 0.37 U/mL (Fig. 4B, b). These results were comparable to that obtained from some reported electrochemical methods such as graphene oxide combining with restriction endonuclease (0.05 U/mL)[35] and enzymatic amplification (0.04 U/mL).[36] It was obviously superior to most of the previously reported methods such as the HRP mimicking DNAzyme (0.4 U/mL)[37] and DNA-functionalized AuNPs amplification (0.12 U/mL).[38]

Selectivity, applicability, accuracy, and precision of the method

To investigate the selectivity of the proposed method, Dam MTase was selected as an interference enzyme, which could methylate all adenine residues within the double stranded recognition sequence of 5′-GATC-3′. Due to the specific site recognition of M.SssI toward its substrate, the proposed method could easily discriminate M.SssI from Dam. As shown in Fig. 4C, significant DPV enhancement was observed in the presence of M.SssI, while no distinct DPV signal was observed in the presence of Dam. These results demonstrated that the electrochemical strategy for M.SssI activity detection exhibited a good selectivity.

A significant and challenging factor for enzyme activity analysis was the applicability in complex biological matrixes. Standardized human serum (diluted in 1:20 ratio with the MTase work buffer) samples spiked with 0.3, 0.6, 0.9, 3, 6, and 9 U/mL M.SssI MTase, respectively, were analyzed using the proposed method. Results were showed in Table 1. Recoveries were from 95.7% to 106.7% and the relative standard derivations were in the range of 4.02% ~ 5.67%, indicating that the method had good accuracy and high precision. Therefore, these results indicated that the proposed strategy held great potential for clinical applications.

Evaluation of DNA MTase inhibitor

In order to demonstrate the validity of our method in evaluating the inhibitors of M.SssI, two kinds of compounds were selected as model inhibitors, such as 5-Aza and procaine, which were representative drugs and have been used in the majority of methylation inhibition experiments and in a large number of clinical trials.[39,40]

Table 1
Recovery of M.*Sss*I MTase added in human serum samples.[a]

Added (U/mL)	Found (U/mL)	Recovery (%)	RSD (%, n = 5)
0.3	0.32	106.7	5.67
0.6	0.61	101.7	4.02
0.9	0.88	97.8	5.15
3.0	2.87	95.7	5.56
6.0	5.79	96.5	4.95
9.0	9.22	102.4	4.19

[a]Human serum samples were obtained from healthy donors at the second hospital of Nanjing. All experiments were performed in compliance with the relevant laws and institutional guidelines issued by the ethical committee of the second hospital of Nanjing. The ethical committee had approved the experiments and informed consent was obtained for any experimentation with human subjects.

Firstly, we evaluated the influences of the inhibitors on HpaII activity. Experiments were performed by cleaving the DTP/target DNA hybrids with 50 U/mL HpaII for 3 h in the presence of different concentrations of the inhibitors (5-Aza or procaine). Results indicated that the two drugs had no obvious influence on the activity of HpaII when the concentration of 5-Aza and procaine was less than 300 and 400 μM, respectively. Then, we evaluated the inhibited effects of the two drugs on M.SssI activity at various concentrations. The activity of the M.SssI decreased with the increasing concentration of 5-Aza and procaine (Fig. 4D), indicating significant dose-dependent inhibition of the methylation of genomic DNA by 5-Aza and procaine. The inhibition efficiency (%) was evaluated as follows: Inhibition (%) = $(I_3-I_2)/(I_3-I_1)*100\%$, where I_1 was the peak current of PANI obtained from DTP/target DNA hybrids modified gold electrode system treated with HpaII. I_2 was the inhibited current of PANI obtained from DTP/target DNA hybrids modified gold electrode with M.SssI, inhibitors, and HpaII. I_3 was the peak current of PANI obtained from DTP/target DNA hybrids modified gold electrode system with M.SssI and HpaII. The IC_{50} value, the inhibitor concentration required to reduce enzyme activity by 50%, was acquired from the plots of relative activity of M.SssI versus the inhibitors concentration and was found to be ~ 58 and 390 μM for 5-Aza and procaine, respectively, which was in agreement with the previously reported result.[41] These results indicated that the developed method had a potential application in studying the inhibited effects of anticancer drugs on MTase and for screening MTase inhibitors.

3. Conclusions

In summary, we have developed a label-free electrochemical platform for assay DNA MTase activity via DNA tetrahedron-structured probe. This method can detect M.SssI activity as low as 0.03 U/mL, with a detection range from 0.05 to 10 U/mL. The good performance of the sensor is ascribed to (1) the DNA tetrahedron controlled the nanospacing between the capture DNA, which greatly improves hybridization efficiency and MTase combination capability; (2) tetrahedral-structure probe supplies abundant nucleic acid backbones for aniline polymerization, which also increases the DPV signal sharply. In addition, the proposed method has been used to evaluate and screen the inhibition of MTase activity. Therefore our method has the potential to be applied for cancer diagnosis and drug development.

Acknowledgements

The project was supported by the Preventive Medicine Research Program of Jiangsu Provincial Health Department (grant no. Y2013001).

References

1 F. Schmitt, E. J. Oakeley and J. P. Jost, *J. Biol. Chem.*, 1997, **272**, 1534−1540.
2 D. M. Heithoff, R. L. Sinsheimer, D. A. Low and M. J. Mahan, *Science*, 1999, **284**, 967−970.
3 K. D. Robertson, *Nat. Rev. Genet.*, 2005, **6**, 597−610.

4 T. M. Geiman and K. Muegge, *Mol. Reprod. Dev.*, 2010, **77**, 105–113.
5 M. Esteller, *Adv. Exp. Med. Biol.*, 2003, **532**, 39–49.
6 Y. Kondo and J. P. Issa, *Expert Rev. Mol. Med.*, 2010, **12**, e23.
7 B. Richardson, *Ageing Res. Rev.*, 2003, **2**, 245–261.
8 M. Esteller, Curr. *Opin. Oncol.*, 2005, **17**, 55–60.
9 W. Li, Z. L. Liu, H. Lin, Z. Nie, J. H. Chen, X. H. Xu and S. Z. Yao, *Anal. Chem.*, 2010, **82**, 1935–1941.
10 Y. X. Zhao, Li. Q, F. Chen, Y. Zhao and C. H. Fan, *Biosens. Bioelectron.*, 2013, **41**, 764–770.
11 Y. P. Zeng, J. Hu, Y. Long and C. Y. Zhang, *Anal. Chem.*, 2013, **85**, 6143–6150.
12 W. Q. Yang, X. Zhu, Q. D. Liu, Z. Y. Lin, B. Qiu and G. N. Chen, *Chem. Commun.*, 2011, **47**, 3129–3131.
13 W. J. Wang, J. J. Li, K. Rui, P. P. Gai, J. R. Zhang and J. J. Zhu, *Anal. Chem.*, 2015, **87**, 3019–3026.
14 H. F. Zhao, R. P. Liang, J. W. Wang and J. D. Qiu, *Biosens. Bioelectron.*, 2015, **63**, 458–464.
15 J. W. Zhou, X. H. Zhang, E. H. Xiong, P. Yu and J. H. Chen, *Chem. Commun.*, 2015, **51**, 5081–5084.
16 S. Pal, Z. T. Deng, B. Q. Ding, H. Yan and Y. Liu, *Angew. Chem. Int. Ed.*, 2010, **49**, 2700–2704.
17 Z. Jin, W. Sun, Y. Ke, C. J. Shih, G. L. C. Paulus, Q. H. Wang, B. Mu, P. Yin and M. S. Strano, *Nat. Commun.*, 2013, **4**, 1663.
18 J. L. Fu, M. H. Liu, Y. Liu, N. W. Woodbury and H. Yan, *J. Am. Chem. Soc.*, 2012, **134**, 5516–5519.
19 Y. L. Wen, H. Pei, Y. Wan, Y. Su, Q. Huang, S. P. Song and C. H. Fan, *Anal. Chem.*, 2011, **83**, 7418–7423.
20 Z. L. Ge, M. H. Lin, P. Wang, H. Pei, J. Yan, J. Y. Sho, Q. Huang, D. N. He, C. H. Fan and X. L. Zuo, *Anal. Chem.*, 2014, **86**, 2124–2130.
21 M. H. Lin, Y. L. Wen, L. Y. Li, H. Pei, G. Liu, H. Y. Song, X. L. Zuo, C. H. Fan, and Q. Huang, *Anal. Chem.*, 2014, **86**, 2285–2288.
22 G. B. Zhou, M. H. Lin, P. Song, X. Q. Chen, J. Chao, L. H. Wang, Q. Huang, W. Huang, C. H. Fan and X. L. Zuo, *Anal. Chem.*, 2014, **86**, 7843–7848.
23 X. Q. Chen, G. B. Zhou, P. Song, J. J. Wang, J. M. Gao, J. X. Lu, C. H. Fan and X. L. Zuo, *Anal. Chem.*, 2014, **86**, 7337–7342.
24 Q. W. Tang, J. H. Wu, X. M. Sun, Q. H. Li and J. M. Lin, *Langmuir*, 2009, **25**, 5253–5257.
25 S. H. Chen, Y. J. Li and Y. L. Li, *Polym. Chem.*, 2013, **4**, 5162–5180.
26 Z. G. Wang, P. F. Zhan and B. Q. Ding, *ACS Nano*, 2013, **7**, 1591–1598.
27 Z. G. Wang, Q. Liu and B. Q. Ding, *Chem. Mater.*, 2014, **26**, 3364–3367.
28 M. Luo, X. Chen, G. H. Zhou, X. Xiang, L. Chen, X. H. Ji and Z. K. He, *Chem. Commun.*, 2012, **48**, 1126–1128.
29 T. Hou, X. J. Liu, X. Z. Wang, A. W. Jiang, S. F. Liu and F. Li, *Sens. Actuators, B: Chem.*, 2014, **190**, 384–388.
30 P. Travascio, Y. F. Li and D. Sen, *Chem. Biol.*, 1998, **5**, 505–517.
31 W. W. Zhao, Z. Y. Ma, P. P. Yu, X. Y. Dong, J. J. Xu and H. Y. Chen, *Anal. Chem.*, 2012, **84**, 917–923.
32 Q. L. Sheng, J. Wang, J. B. Zheng, Z. Q. Xu and H. F. Zhang, *Biosens. Bioelectron.*, 2010, **25**, 2071–2077.
33 M. H. Lin, J. J. Wang, G. B. Zhou, J. B. Wang, N. Wu, J. X. Lu, J. M. Gao, X. Q. Chen, J. Y. Shi, X. L. Zuo and C. H. Fan, *Angew. Chem. Int. Ed.*, 2015, **54**, 2151–2155.
34 R. Wacker, H. Schroder and C. M. Niemeyer, *Anal. Biochem.*, 2004, **330**, 281–287.
35 W. Li, P. Wu, H. Zhang and C. X. Cai, 2012, *Anal. Chem.*, **84**, 7583–7590.
36 H. W. Wu, S. C. Liu, J. H. Jiang, G. L. Shen and R. Q. Yu, *Chem. Commun.*, 2012, **48**, 6280–6282.
37 Y. X. Zhao, F. Chen, M. L. Lin and C. H. Fan, *Biosens. Bioelectron.*, 2014, **54**, 565–570.
38 X. X. He, J. Su, Y. H. Wang, K. M. Wang, X. Q. Ni and Z. F. Chen, *Biosens. Bioelectron.*, 2011, **28**, 298–303.
39 C. Stresemann, B. Brueckner, T. Musch, H. Stopper and F. Lyko, *Cancer Res.*, 2006, **66**, 2794–2800.
40 J. K. Christman, *Oncogene*, 2002, **21**, 5483–5495.
41 M. Wang, Z. N. Xu, L. J. Chen, H. S. Yin and S. Y. Ai, *Anal. Chem.*, 2012, **84**, 9072–9078.

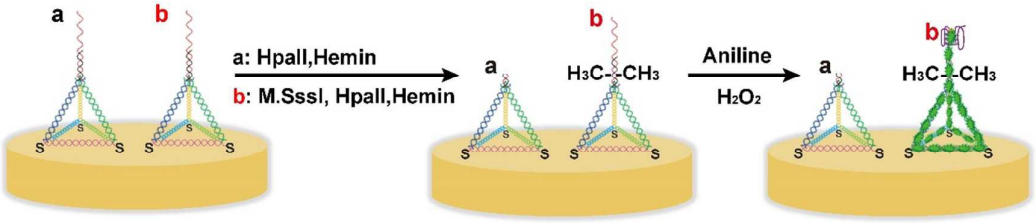

Label-free electrochemical detection of DNA methyltransferase activity *via* DNA tetrahedron-structured probe.